Int. J. Heat Mass Transfer. Vol. 31, No. 9, pp. 1899–1911, 1988
Printed in Great Britain

0017–9310/88 $3.00 + 0.00

ITPE technique applications to time-varying two-dimensional ground-coupling problems

MONCEF KRARTI,† DAVID E. CLARIDGE‡ and JAN F. KREIDER†

†Joint Center for Energy Management, CEAE Department, University of Colorado, Boulder, CO 80309-0428, U.S.A.

‡Department of Mechanical Engineering, Texas A&M University, College Station, TX 77843-3123, U.S.A.

(*Received* 18 *August* 1987 *and in final form* 8 *February* 1988)

Abstract—The interzone temperature profile estimation (ITPE) procedure is used to find two-dimensional analytical series solutions for the time-varying heat transfer between ground and slab-on-grade floors or basements. The undisturbed soil temperature is approximated as a sinusoidal function of time and the ITPE procedure is coupled with the complex temperature technique to derive the steady-periodic solutions for both configurations. The influence of insulation and of a fixed-temperature water table on the temporal behavior of slab-on-grade floors and basements is treated analytically for the first time.

1. INTRODUCTION

IN REF. [1], the temperature variation in the soil was analyzed when steady-state conditions were assumed. In this paper, another key parameter will be included in the formulation of the ground-coupling problems treated in ref. [1]. This key parameter is time. In fact, even though the building and water table temperatures are generally constant, the soil temperature varies significantly with time. As analyzed in refs. [2–5], the earth temperature variation with time can be closely approximated by a sinusoidal function at any below-grade depth. The obvious consequence of this temperature fluctuation is to complicate the heat flow direction from the ground-coupled structure since, depending on time and location, the soil surface can be warmer or colder than the building interior. The disturbance in the earth temperature introduced by a structure reaches a steady-periodic behavior after a few months from the date when the structure is built [6]. These first months constitute the 'transient' period of the building. The length of the transient period depends on many factors such as the size, mass and insulation of the building. The *steady-periodic* behavior is characterized by sinusoidal time variation of earth temperature and heat fluxes. In this paper, the steady-periodic behavior will be analyzed for annual fluctuations. However, the theory can be applied for any other period of time.

Over a dozen methods for calculating heat transfer between buildings and ground are now available and have been reviewed by Sterling and Meixel [7] and Claridge [8]. Virtually all of these methods are based on large computer programs using numerical techniques such as finite differences or finite elements. Most of the existing methods quantify the annual variation of heat flow from a ground-coupled structure but give very little physical insight on how heat is exchanged. Very few authors have attempted to develop analytical solutions to earth-contact problems. Due to the mathematical complexity, the available analytical solutions are generally limited to simplified models which do not consider a water table [9] or permit the inclusion of envelope insulation [10].

This paper presents a more realistic model that predicts the annual variation of the heat flow from a rather general ground-coupled structure, sheds some light on how heat flows from buildings to ground and determines the major parameters that affect soil temperature variation and the total amount of heat flow from a building envelope in contact with earth. In this paper, time varying quantities (such as the heat flow) are characterized by a mean, an amplitude, and a phase shift relative to the soil surface temperature. In order to determine these parameters for each building configuration (i.e. a building with slab-on-grade floor, or a rectangular basement), the time-dependent heat conduction equation for the temperature in the ground is solved in each case using the ITPE technique introduced in refs. [1, 11, 12]. The fact that steady-periodic conditions are assumed allows the time-dependent heat conduction equation to be transformed into a Helmholtz-type equation independent of time. This transformation is discussed in Section 2 of this paper. The general procedure for solving the heat conduction equation is also described.

In Section 3, the two-dimensional periodic temperature beneath a slab-on-grade floor is treated. Also, the dependence of the total floor heat loss upon key parameters is discussed.

Section 4 discusses the two dimensional steady-periodic conduction solution around an insulated rectangular basement. The heat loss from the walls and the floor is determined and the effect of insulation levels on the total heat loss is shown.

NOMENCLATURE

a half width of ground-coupled building [m]
A_n, B_n, C_n general term in Fourier series temperature expansion
A'_n, B'_n, C'_n general term in Fourier series heat flow expansion
b water table depth [m]
c basement depth [m]
f, g functions of one of the space coordinates [K]
f_n, g_n Fourier coefficients
H ratio, h/k_s [m^{-1}]
h overall heat transfer conductance [$W m^{-2} K^{-1}$]
I heat flux [$W m^{-2}$]
$\mathscr{I}$ complex heat flux amplitude, $(1+i)$ [$W m^{-2}$]
k_s soil thermal conductivity [$W m^{-1} K^{-1}$]
L distance from building center to a boundary where soil temperature is undisturbed [m]
Q total heat loss [$W m^{-1}$]
$\mathscr{Q}$ complex total heat loss amplitude, $(1+i)$ [$W m^{-1}$]
Re real part of a complex number
T temperature [K]
T_m annual mean of soil surface temperature [K]
T_v annual amplitude of soil surface temperature variation [K]
$\mathscr{T}$ complex temperature amplitude, $K+iK$
$\mathscr{T}_i$ complex room air temperature amplitude, $K+iK$
$\mathscr{T}_w$ complex water table temperature amplitude, $K+iK$
$\mathscr{T}_1$ complex soil surface temperature amplitude, $K+iK$
t time [s]
x, y space coordinates [m].

Greek symbols
$\alpha_p, \beta_{m,p}$ coefficients defined in equation (11)
$\alpha^f_{n,p}, \beta^f_{n,p}, \gamma^f_p$ coefficients defined in equation (21)
$\alpha^g_{n,p}, \beta^g_{n,p}, \gamma^g_p$ coefficients defined in equation (23)
δ complex variable defined in equation (4), $(1+i)$ [m]
$\zeta_n, \chi_n, \nu_n, \mu_n$ eigenvalues
$\zeta'_n, \chi'_n, \nu'_n, \mu'_n$ complex eigenvalues
κ_s soil thermal diffusivity [$m^2 s^{-1}$]
θ complex temperature amplitude, $(1+i)$ [K]
ω angular frequency for annual cycle, 1.992×10^{-7} rad s^{-1}.

Subscripts
f floor
s mean
t amplitude
wl walls
I zone (I)
II zone (II)
III zone (III).

2. GENERAL SOLUTION PROCEDURE

The time-dependent heat conduction equation in an isotropic medium is given by the following equation [4]:

$$\Delta T(\mathbf{r}, t) = \frac{1}{\kappa_s} \frac{\partial T(\mathbf{r}, t)}{\partial t} \tag{1}$$

where Δ is the Laplacian operator. Throughout this section, Δ will be assumed to be given in the two-dimensional Cartesian form, i.e.

$$\Delta = \frac{\partial^2}{\partial x^2} + \frac{\partial^2}{\partial y^2}.$$

The coordinates x and y are denoted by the vector space $\mathbf{r}$ (i.e. $\mathbf{r} = (x, y)$). In equation (1), t is time and κ_s the soil thermal diffusivity. Note that under practical conditions, the soil thermal properties are not quite constant and are greatly complicated in the presence of water [13]. A theory based on the assumption of constant diffusivity can only give approximate results.

In steady-periodic conditions, the solution $T(\mathbf{r}, t)$ of equation (1) can be found by applying the complex temperature technique [4]. $T(\mathbf{r}, t)$ is then in the form

$$T(\mathbf{r}, t) = T_s(\mathbf{r}) + \mathrm{Re}\,[T_t(\mathbf{r})\, e^{i\omega t}]. \tag{2}$$

In the above equation, T_s is the mean of the periodic temperature variation over the annual cycle and T_t is the *complex* amplitude of the annual temperature fluctuations. A real amplitude and a phase shift can be obtained by taking the modulus and the argument of the complex value of T_t, respectively. The symbol ω represents the angular frequency of the annual cycle and is equal to 1.992×10^{-7} rad s^{-1}.

In a previous work [11], it was shown that both $T_s(\mathbf{r})$ and $T_t(\mathbf{r})$ can be deduced from a complex temperature solution $\mathscr{T}(\mathbf{r})$ of the following Helmholtz equation:

$$\Delta \mathscr{T}(\mathbf{r}) = \delta^2 \mathscr{T}(\mathbf{r}) \tag{3}$$

with

$$\delta = \sqrt{\left(\frac{i\omega}{\kappa_s}\right)}. \tag{4}$$

The boundary conditions specific to each problem have to be considered to determine the solution $\mathscr{T}(\mathbf{r})$. The boundary conditions also determine the manner by which T_s and T_t are deduced from $\mathscr{T}$. For the steady-state component T_s, one additionally substitutes zero for δ in the expression for $\mathscr{T}$.

To solve equation (1) for each of the two ground-coupling problems treated here, the following steps are taken.

(1) The solution $\mathscr{T}(\mathbf{r})$ of the Helmholtz equation (3) is found.

(2) The expressions for the steady-state temperature $T_s(\mathbf{r})$ and the complex temperature amplitude $T_t(\mathbf{r})$ are deduced from the solution $\mathscr{T}(\mathbf{r})$ using appropriate boundary conditions.

(3) Finally, the time-dependent temperature solution $T(\mathbf{r}, t)$ of equation (1) is determined from equation (2).

In this paper the first step is emphasized. It is then relatively easy to carry out the remaining two steps.

3. INSULATED SLAB-ON-GRADE FLOOR

The complex temperature amplitude $\mathscr{T}(x, y)$ for an insulated slab-on-grade floor configuration shown in Fig. 1 is subject to the following equation:

$$\Delta\mathscr{T} = \delta^2\mathscr{T} \tag{5}$$

with

$$\mathscr{T} = \mathscr{T}_w \qquad \text{for } y = b$$

$$\mathscr{T} = \mathscr{T}_1 \qquad \text{for } y = 0 \text{ and } |x| > a$$

$$\frac{\partial\mathscr{T}}{\partial y} = H(\mathscr{T} - \mathscr{T}_i) \qquad \text{for } y = 0 \text{ and } |x| < a.$$

To clarify the values of $\mathscr{T}_i$, $\mathscr{T}_1$ and $\mathscr{T}_w$ to be used in the above equations, consider an example of a building interior kept at 18°C throughout the year. The floor of this building is adjacent to a soil surface with an annual temperature fluctuation from 1 to 15°C. Beneath this floor, there is a water table at a constant temperature of 10°C.

For this example, the mean of the annual temperature variation T_s is the solution of equation (5) with $\delta = 0$, $\mathscr{T}_w = 10$°C, $\mathscr{T}_1 = 8$°C and $\mathscr{T}_i = 18$°C. The complex amplitude T_t is also a solution of equation (5) but with the amplitudes $\mathscr{T}_w = 0$°C, $\mathscr{T}_1 = 7$°C and $\mathscr{T}_i = 0$°C. Therefore, the variation of the temperatures $(\mathscr{T}_w; \mathscr{T}_1; \mathscr{T}_i)$ at the soil boundaries determine the manner by which T_s and T_t are obtained from the formal expression for $\mathscr{T}$, the solution of equation (5).

To find the formal expression for $\mathscr{T}(x, y)$, we first note that equation (5) is equivalent to the following equation:

$$\Delta\theta = \delta^2\theta \tag{6}$$

with

$$\theta = 0 \qquad \text{for } y = b$$

$$\theta = \theta_1 \qquad \text{for } y = 0 \text{ and } |x| > a$$

$$\frac{\partial\theta}{\partial y} = H(\theta - \theta_i) \qquad \text{for } y = 0 \text{ and } |x| < a$$

where

$$\theta(x, y) = \mathscr{T}(x, y) - \mathscr{T}_w e^{\delta(y-b)}$$

$$\theta_1 = \mathscr{T}_1 - \mathscr{T}_w e^{-\delta b}$$

$$\theta_i = \mathscr{T}_i - \mathscr{T}_w e^{-\delta b}(1 - \delta/H). \tag{7}$$

Note that for steady conditions (i.e. when $\delta = 0$) the above transformation establishes $\mathscr{T}_w$ as the origin of temperatures.

Now let us solve the Helmholtz equation stated in equation (6) using the ITPE technique. Referring to Fig. 1 and because of the symmetry around the axis $x = 0$, the temperature $\theta(x, y)$ needs to be determined only in zones (I) and (II). The function $f(y)$ denotes the temperature profile along the surface $x = -a$. The solution of equation (6) in zone (I) is

$$\theta_I(x, y) = \frac{2}{b}\sum_{n=1}^{\infty}\frac{\sin \nu_n y}{\nu_n} \times \left\{\frac{\nu_n}{\nu_n'}\theta_1[1 - e^{\nu_n'(x+a)}] + \nu_n f_n e^{\nu_n'(x+a)}\right\}. \tag{8}$$

In zone (II), the temperature $\theta_{II}(x, y)$ is given by

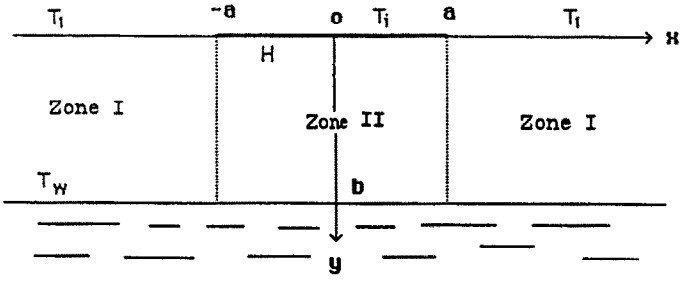

FIG. 1. Slab-on-grade floor configuration.

$$\theta_{II}(x,y) = \frac{2}{b}\sum_{n=1}^{\infty} f_n \sin \nu_n y \frac{\cosh \nu'_n x}{\cosh \nu'_n a} - \frac{2}{a}\sum_{n=1}^{\infty} (-1)^n C_n \cos \mu_n x \frac{\sinh \mu'_n (b-y)}{\sinh \mu'_n b} \quad (9)$$

where

$$\nu_n = \frac{n\pi}{b}, \quad \nu'_n = \sqrt{(\nu_n^2 + \delta^2)}$$

$$f_n = \int_0^b f(y) \sin \nu_n y \, dy$$

$$\mu_n = \frac{(2n-1)\pi}{2a}, \quad \mu'_n = \sqrt{(\mu_n^2 + \delta^2)}$$

and

$$C_n = \frac{H\theta_i/\mu_n + \frac{2}{b}\sum_{m=1}^{\infty} f_m \mu_n \nu_m / (\mu'^2_n + \nu_m^2)}{(H + \mu'_n \coth \mu'_n b)}.$$

The continuity of heat flux at the surface $x = -a$ gives the condition

$$\left.\frac{\partial \theta_I}{\partial x}\right|_{x=-a} = \left.\frac{\partial \theta_{II}}{\partial x}\right|_{x=-a} \quad (10)$$

or

$$\frac{2}{b}\sum_{n=1}^{\infty} \sin \nu_n y \left(\nu'_n f_n - \frac{\nu_n}{\nu'_n}\theta_1\right) = \frac{-2}{b} \times \sum_{n=1}^{\infty} \nu'_n \tanh \nu'_n a \, f_n \sin \nu_n y + \frac{2}{a}\sum_{n=1}^{\infty} \mu_n C_n \frac{\sinh \mu'_n (b-y)}{\sinh \mu'_n b}.$$

In order to obtain the Fourier coefficients f_n, let us multiply the above equality by $\sin \nu_p y$ $(p = 1, 2, \ldots)$ and integrate the resultant equation over $[0, b]$. After rearrangement, it is found that the coefficients f_p are solutions of the following linear systems:

$$f_p = \alpha_p + \sum_{m=1}^{\infty} \beta_{m,p} f_m \quad (11)$$

where

$$\alpha_p = \frac{1}{\nu'_p (1 + \tanh \nu'_p a)}\left[\frac{\nu_p}{\nu'_p}\theta_1 + \frac{2}{a}\sum_{n=1}^{\infty} \frac{H\theta_i \nu_p}{(H + \mu'_n \coth \mu'_n b)(\mu'^2_n + \nu_p^2)}\right]$$

and

$$\beta_{m,p} = \frac{4\nu_p \nu_m}{ab\nu'_p (1 + \tanh \nu'_p a)} \times \sum_{n=1}^{\infty} \frac{\mu_n^2}{(H + \mu'_n \coth \mu'_n b)(\mu'^2_n + \nu_p^2)(\mu'^2_n + \nu_m^2)}.$$

As done in ref. [1] for the case of steady-state temperature variation, the sum in equation (11) is truncated to $N = 15$ terms and the f_p's are determined by using the Gauss–Jordan elimination method. Note that the Fourier coefficients f_p have complex arguments for the solution T_t but they are real numbers for the solution T_s. The profile f can be solved for as exactly as desired depending on how many Fourier coefficients f_p are determined. This new technique is more precise than the estimation technique originally used in refs. [11, 12].

3.1. *Soil temperature variation*

Figure 2 shows the temperature distribution beneath a slab floor of half width $a = 3$ m and an insulation such that $h = 1\ \mathrm{W\,m^{-2}\,°C^{-1}}$. A water table at $T_w = 10°C$ is $b = 5$ m below grade. Throughout the year, the interior temperature is assumed to be constant at $T_i = 18°C$, while the soil surface temperature fluctuates around a mean $T_m = 8°C$ with an amplitude $T_v = 7°C$. The soil thermal diffusivity is taken to be $\kappa_s = 6.45 \times 10^{-7}\ \mathrm{m^2\,s^{-1}}$. The soil temperature variations are illustrated for two different dates of the year.

The summertime profile, when the soil surface temperature is at its peak (here 15°C) is shown in Fig. 2(a). Throughout this paper, it will be assumed that the soil surface temperature reaches its maximum on 15 July. For the floor configuration chosen in Fig. 2, the water table acts as a heat sink for both the slab floor and the soil surface since it has the lowest temperature among the three surfaces during the summertime. However, the slab does not lose its entire heat to the water table. In fact, part of this heat goes to the soil surface through the slab edges.

In wintertime (around 15 January), the ground temperature profile changes completely as shown in Fig. 2(b). Now, the soil surface receives heat from both the water table and the slab floor since its temperature has dropped to 1°C. At the water table surface, two double points [1] appear (symmetric to each other). These double points divide the water table into two zones, a *warm* zone beneath the slab receiving heat and a *cold* zone losing heat as noted in ref. [1].

It is clear that for the specific slab-on-grade case of Fig. 2 the floor loses heat to both the soil surface and the water table throughout the year. It is the proportion of the heat lost to each surface that fluctuates with time. In wintertime, the floor loses more heat to the soil surface than to the water table. It is the converse situation in summertime but the total heat losses from the slab are less important during this period.

Figure 3(a) shows the steady-state soil temperature for the above case. These profiles represent the term T_s in equation (2). They are calculated from equations (8) and (9) by setting $\delta = 0$; $\mathscr{T}_i = 18°C$; $\mathscr{T}_w = 10°C$ and $\mathscr{T}_1 = 8°C$. The variations of the real part of the term T_t are shown in Fig. 3(b). It is determined from the same equations (8) and (9) by letting $\mathscr{T}_i = \mathscr{T}_w = 0°C$ and $\mathscr{T}_1 = 7°C$. Note that just below the floor central area the real amplitude of the soil temperature is almost zero, implying that at these locations the temperature is nearly constant throughout the year. The same applies for the zone of the ground just above the water table.

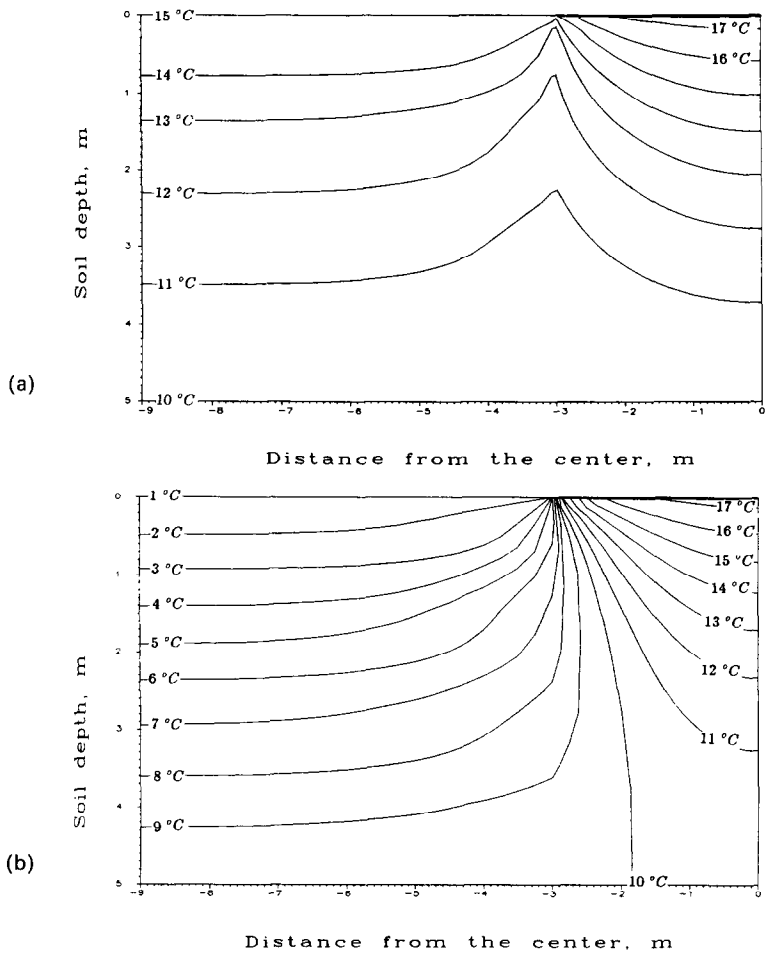

FIG. 2. Earth temperature isotherms beneath an insulated slab-on-grade floor with $T_i = 17°C$, $T_1 = 8 + 7\cos\omega t$ (°C), $T_w = 10°C$ for: (a) summertime (15 July); (b) wintertime (15 January).

3.2. *Total slab heat losses*

The complex amplitude of the total floor heat losses $\mathcal{Q}(\delta)$ is obtained by integrating the complex heat flux $\mathcal{J}(x) = h(\mathcal{T}(x,0) - \mathcal{T}_i)$ over $[0, b]$

$$\mathcal{Q}(\delta) = 2ak_s\delta T_w e^{-\delta b} - \frac{4}{a}h\sum_{n=1}^{\infty} C'_n \qquad (12)$$

with

$$C'_n = \mu'_n\theta_i \coth \mu'_n b/\mu_n - \frac{2}{b}\sum_{m=1}^{\infty}\frac{\mu_n\nu_m f_m/(\nu_m^2+\mu_n'^2)}{(H+\mu'_n\coth\mu'_n b)}.$$

Again the time-dependent total floor heat loss $Q(t)$ is calculated from an equation similar to equation (2)

$$Q(t) = \mathcal{Q}(0) + \mathrm{Re}[\mathcal{Q}(\delta)e^{i\omega t}]. \qquad (13)$$

Figures 4(a) and (b) show the fluctuations of the total floor heat losses $Q(t)$ during one year for a slab width $2a = 6$ m with

$$\kappa_s = 6.45\times10^{-7}\ \mathrm{m^2\,s^{-1}},\quad k_s = 1\ \mathrm{W\,m^{-1}\,°C^{-1}}$$

$$T_i = 18°C,\quad T_1 = 8+7\cos\omega t\ (°C),\quad T_w = 10°C.$$

The effect of varying the water table depth is shown for two floor insulation levels ($h = 1$ W m^{-2} °C^{-1} in Fig. 4(a) and $h = 5$ W m^{-2} °C^{-1} in Fig. 4(b)). As one could expect, the total floor heat loss decreases as the insulation increases. Also, the phase lag between the soil surface temperature and the total losses increases as the insulation increases (i.e. h decreases) particularly when $b = 5$ m. In the case of $b = 1$ m, the water table has a damping effect on the floor heat loss fluctuations. In fact, the amplitude of the variations of $Q(t)$ decreases as b decreases while the annual mean Q_s increases. This behavior is related to the fact that the water table is at constant temperature (10°C). Therefore, as b decreases the heat flow pattern from the slab approaches that occurring for two parallel planes at two different constant temperatures.

4. INSULATED RECTANGULAR BASEMENT

The model of Fig. 5 will be used to treat the rectangular basement configuration. Along the bounding surfaces $x = \pm L$, the soil temperature is undisturbed. The expression of the complex amplitude of the undisturbed soil temperature is given by

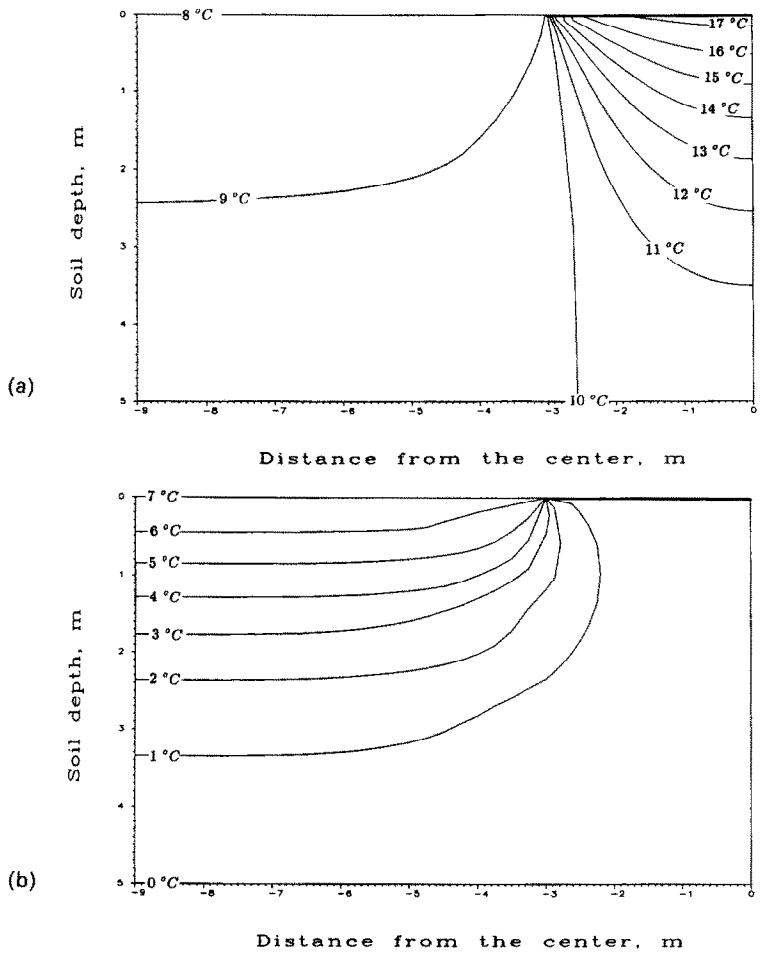

FIG. 3. Earth temperature isotherms beneath an insulated slab-on-grade floor with: (a) $T_i = 17°C$, $T_1 = 8°C$, $T_w = 10°C$; (b) $T_i = T_w = 0°C$, $T_1 = 7°C$.

$$\mathcal{T}(\pm L, y) = \mathcal{T}_L(y) = \mathcal{T}_w \frac{\sinh \delta y}{\sinh \delta b} + \mathcal{T}_1 \frac{\sinh \delta(b-y)}{\sinh \delta b}. \quad (14)$$

In these conditions the complex temperature distribution $\mathcal{T}(x, y)$, around the rectangular basement is the solution of the following equation:

$$\Delta \mathcal{T} = \delta^2 \mathcal{T} \quad (15)$$

$$\frac{\partial \mathcal{T}}{\partial y} = H_f(\mathcal{T} - \mathcal{T}_i) \quad \text{for } y = c \text{ and } |x| < a$$

$$\frac{\partial \mathcal{T}}{\partial x} = H_{wl}(\mathcal{T}_i - \mathcal{T}) \quad \text{for } y < c \text{ and } |x| = a$$

$$\mathcal{T} = \mathcal{T}_1 \quad \text{for } y = 0 \text{ and } |x| > a$$

$$\mathcal{T} = \mathcal{T}_L(y) \quad \text{for } |x| = L$$

$$\mathcal{T} = \mathcal{T}_w \quad \text{for } y = b$$

where $H_f = h_f/k_s$ and $H_{wl} = h_{wl}/k_s$. h_f and H_{wl} are the values of the air-to-soil conductance at the floor and at the walls, respectively.

To solve the Helmholtz equation, equation (15), by the ITPE technique, we will determine the temperature variation in zones (I), (II), and (III) as defined in Fig. 5. The temperature profiles at the surfaces $x = -a$ and $y = c$ are functions of y and x, respectively

$$\mathcal{T}(-a, y) = f(y), \qquad c < y < b$$

and

$$\mathcal{T}(x, c) = g(x), \quad -L < x < -a.$$

The separation of variables technique yields the solution in zone (I)

$$\mathcal{T}_I(x, y) = \frac{2}{(b-c)} \sum_{n=1}^{\infty} f_n \sin \nu_n (y-c) \frac{\cosh \nu'_n x}{\cosh \nu'_n a} - \frac{2}{a} \mathcal{T}_w \sum_{n=1}^{\infty} \frac{(-1)^n}{\mu_n} \cos \mu_n x \frac{\sinh \mu'_n (y-c)}{\sinh \mu'_n (b-c)} + \frac{2}{a} \sum_{n=1}^{\infty} A_n \cos \mu_n x \frac{\sinh \mu'_n (b-y)}{\sinh \mu'_n (b-c)}. \quad (16)$$

In zone (III), the solution is

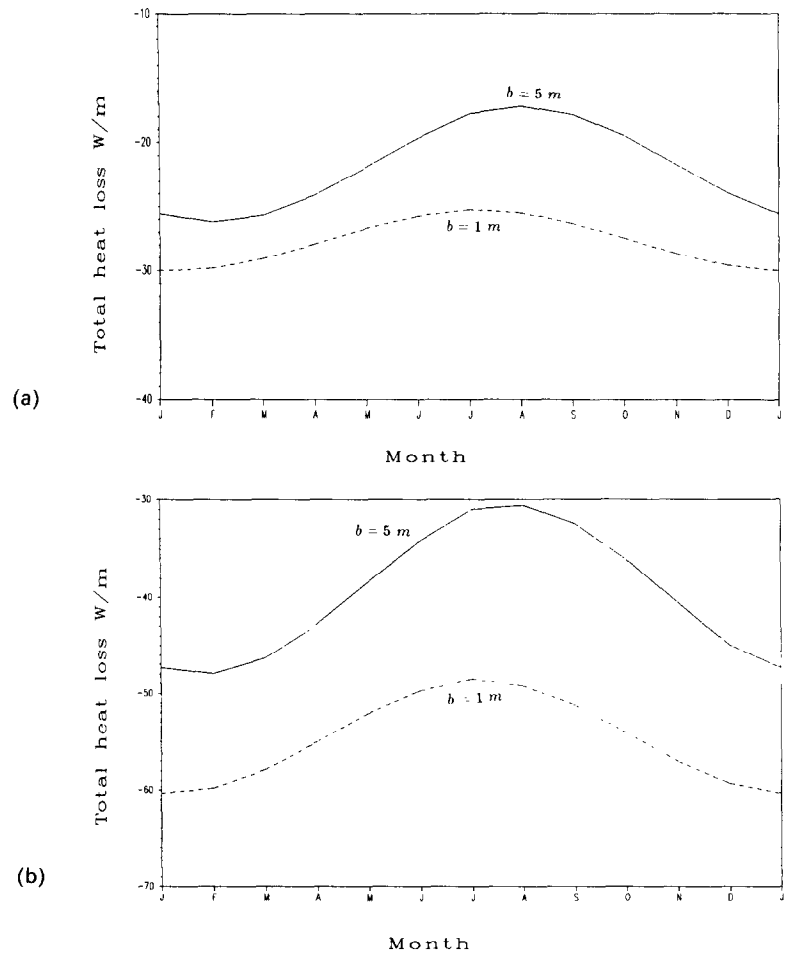

FIG. 4. Effect of water table depth on the annual variation of total slab heat losses: (a) $H = 1\ \mathrm{m}^{-1}$; (b) $H = 5\ \mathrm{m}^{-1}$.

$$\mathscr{T}_{\mathrm{III}}(x,y) = \frac{2}{(L-a)}\sum_{n=1}^{\infty} g_n \sin\chi_n(x+a)\frac{\sinh\chi'_n(b-y)}{\sinh\chi'_n(b-c)} - \frac{2}{(L-a)}\mathscr{T}_{\mathrm{w}}\sum_{n=1}^{\infty}\frac{[1-(-1)^n]}{\chi_n}\sin\chi_n(x+a) \times \frac{\sinh\chi'_n(y-c)}{\sinh\chi'_n(b-c)} + \frac{2}{(b-c)}\sum_{n=1}^{\infty} f_n \sin\nu_n(y-c) \times \frac{\sinh\nu'_n(x+L)}{\sinh\nu'_n(L-a)} + \frac{2}{(b-c)}\sum_{n=1}^{\infty}\frac{B_n}{\nu_n}\sin\nu_n(y-c) \times \frac{\sinh\nu'_n(x+a)}{\sinh\nu'_n(a-L)}. \quad (17)$$

The expression for the temperature in zone (II) takes the form

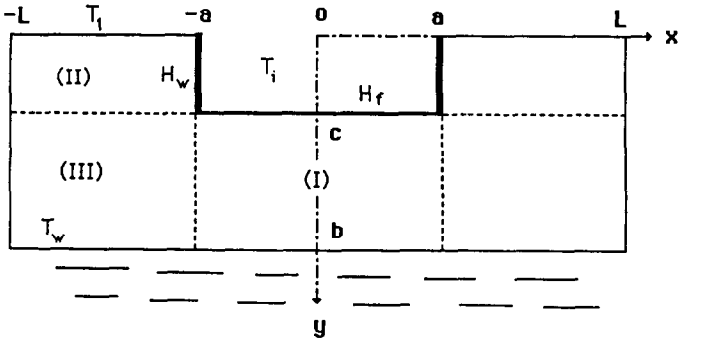

FIG. 5. Rectangular basement configuration with finite water table level.

$$\mathscr{T}_{II}(x,y) = \frac{2}{(L-a)}\mathscr{T}_1 \sum_{n=1}^{\infty} \frac{[(-1)^n-1]}{\chi_n}\sin\chi_n(x+a) \times \frac{\sinh\chi_n'(c-y)}{\sinh\chi_n'c} + \frac{2}{(L-a)}\sum_{n=1}^{\infty} g_n \sin\chi_n(x+a) \times \frac{\sinh\chi_n' y}{\sinh\chi_n' c} + \frac{2}{c}\sum_{n=1}^{\infty} C_n \sin\zeta_n y \frac{\sinh\zeta_n'(x+a)}{\sinh\zeta_n'(a-L)} + \frac{2}{c}\sum_{n=1}^{\infty} D_n \sin\zeta_n y \frac{\sinh\zeta_n'(x+L)}{\sinh\zeta_n'(L-a)} \quad (18)$$

where

$$\nu_n = \frac{n\pi}{(b-c)}; \qquad \nu_n' = \sqrt{(\nu_n^2+\delta^2)}$$

$$\chi_n = \frac{n\pi}{(L-a)}; \qquad \chi_n' = \sqrt{(\chi_n^2+\delta^2)}$$

$$\zeta_n = \frac{n\pi}{c}; \qquad \zeta_n' = \sqrt{(\zeta_n^2+\delta^2)}$$

$$\mu_n = \frac{(2n-1)\pi}{2a}; \qquad \mu_n' = \sqrt{(\mu_n^2+\delta^2)}$$

$$f_n = \int_c^b f(y)\sin\nu_n(y-c)\,dy;$$

$$g_n = \int_{-L}^{-a} g(x)\sin\chi_n(x+a)\,dx$$

$$A_n = -\frac{(-1)^n\{H_f\mathscr{T}_i/\mu_n + \mu_n'\mathscr{T}_w/[\mu_n\sinh\mu_n'(b-c)]\}}{H_f+\mu_n'\coth\mu_n'(b-c)} - \frac{2(-1)^n}{(b-c)}\sum_{m=1}^{\infty}\frac{f_m\nu_m\mu_n/(\nu_m'^2+\mu_n^2)}{H_f+\mu_n'\coth\mu_n'(b-c)}$$

$$B_n = \frac{\nu_n}{\nu_n'^2}\left\{\mathscr{T}_w\left[\frac{\sinh\delta c}{\sinh\delta b}-(-1)^n\right]+\mathscr{T}_1\frac{\sinh\delta(b-c)}{\sinh\delta b}\right\}$$

$$C_n = \frac{\zeta_n}{\zeta_n'^2}\left\{\mathscr{T}_1\left[1-(-1)^n\frac{\sinh\delta(b-c)}{\sinh\delta b}\right] - (-1)^n\mathscr{T}_w\frac{\sinh\delta c}{\sinh\delta b}\right\}$$

$$D_n = \frac{[1-(-1)^n]H_{wl}\mathscr{T}_i/\zeta_n+\zeta_n' C_n/\sinh\zeta_n'(a-L)}{H_{wl}+\zeta_n'\coth\zeta_n'(L-a)} + \frac{\zeta_n\mathscr{T}_1\tanh[\zeta_n'(L-a)/2]/\zeta_n'}{H_{wl}+\zeta_n'\coth\zeta_n'(L-a)} - \frac{2}{(L-a)}\sum_{m=1}^{\infty}\frac{(-1)^n\chi_m\zeta_n g_m/(\chi_m'^2+\zeta_n^2)}{H_{wl}+\zeta_n'\coth\zeta_n'(L-a)}.$$

The Fourier coefficients f_n and g_n can be determined from the required continuity of heat flux along the surfaces $x = -a$ and $y = c$. First, for $x = -a$ flux continuity yields

$$\left.\frac{\partial\mathscr{T}_1}{\partial x}\right|_{x=-a} = \left.\frac{\partial\mathscr{T}_{III}}{\partial x}\right|_{x=-a}. \quad (19)$$

After a computation procedure similar to that followed in the slab-on-grade section, the condition given by equation (19) leads to

$$f_p = \gamma_p^f + \sum_{n=1}^{\infty}\alpha_{n,p}^f f_n + \sum_{n=1}^{\infty}\beta_{n,p}^f g_n \quad (20)$$

with

$$\gamma_p^f = \frac{1}{\nu_p'[\tanh\nu_p'(a)+\coth\nu_p'(L-a)]} \times \left[\frac{2}{a}\sum_{n=1}^{\infty}\frac{\nu_p\mu_n[H_f\mathscr{T}_i/\mu_n+\mu_n'\mathscr{T}_w/\mu_n\sinh\mu_n'(b-c)]}{[H_f+\mu_n'\coth\mu_n'(b-c)](\nu_p^2+\mu_n'^2)} + \left(\frac{\nu_p' B_p}{\sinh\nu_p'(L-a)} - (-1)^p\frac{\nu_p}{\nu_p'}\mathscr{T}_w\{\tanh\nu_p' a + \tanh[\nu_p'(L-a)/2]\}\right)\right]$$

$$\beta_{n,p}^f = -\frac{2}{(L-a)}\frac{1}{\nu_p'[\tanh\nu_p' a+\coth\nu_p'(L-a)]}\frac{\chi_n\nu_p}{\chi_n^2+\nu_p^2}$$

$$\alpha_{n,p} = \sum_{m=1}^{\infty} \times \frac{4\nu_n\nu_p\mu_m^2/a(b-c)(\nu_p^2+\mu_m'^2)(\nu_n'^2+\mu_m^2)}{\nu_p'[H_f+\mu_m'\coth\mu_m'(b-c)][\tanh\nu_p' a+\coth\nu_p'(L-a)]}.$$

The condition of heat flux continuity at the surface $y = c$ is expressed by

$$\left.\frac{\partial\mathscr{T}_{II}}{\partial y}\right|_{y=c} = \left.\frac{\partial\mathscr{T}_{III}}{\partial y}\right|_{y=c}. \quad (21)$$

This condition yields a system of equations of the form

$$g_p = \gamma_p^g + \sum_{m=1}^{\infty}\alpha_{m,p}^g g_m + \sum_{m=1}^{\infty}\beta_{m,p}^g f_m \quad (22)$$

where

$$\gamma_p^g = \frac{1}{\chi_p'[\coth\chi_p' c+\coth\chi_p'(b-c)]} \times \left\{-\frac{\chi_p'}{\chi_p}[1-(-1)^p]\left[\frac{\mathscr{T}_1}{\sinh\chi_p' c}+\frac{\mathscr{T}_w}{\sinh\chi_p'(b-c)}\right] - \frac{2}{c}\sum_{n=1}^{\infty}\frac{(-1)^{n+p}C_n\zeta_n\chi_p}{\chi_p^2+\zeta_n'^2} + \frac{2}{(b-c)}\sum_{n=1}^{\infty}\frac{(-1)^p B_n\nu_n\chi_p}{\chi_p^2+\nu_n'^2} - \frac{2}{c}T_i\sum_{n=1}^{\infty}\frac{[1-(-1)^n]\chi_p H_{wl}}{[H_{wl}+\zeta_n'\coth\zeta_n'(L-a)](\chi_p^2+\zeta_n'^2)} + \frac{2}{c}\sum_{n=1}^{\infty}\frac{(-1)^n\chi_p\zeta_n\zeta_n' C_n/\sinh\zeta_n'(L-a)}{[H_{wl}+\zeta_n'\coth\zeta_n'(L-a)](\zeta_n'^2+\chi_p^2)} + \frac{2}{c}T_1\sum_{n=1}^{\infty}(-1)^n\frac{\zeta_n^2\chi_p\zeta_n'\tanh[\zeta_n'(L-a)/2]}{[H_{wl}+\zeta_n\coth\zeta_n(L-a)](\zeta_n'^2+\chi_p^2)}\right\}$$

$$\alpha_{m,p}^g = \sum_{n=1}^{\infty} \times \frac{4\zeta_n^2\chi_p\chi_m/c(L-a)(\zeta_n'^2+\chi_p^2)(\zeta_n^2+\chi_m'^2)}{\chi'_p[H_{wl}+\zeta_n\coth\zeta_n'(L-a)][\coth\chi_p' c+\coth\chi_p'(b-c)]}$$

$$\beta_{m,p}^g = -\frac{2}{(b-c)}\frac{1}{\chi_p'[\coth\chi_p' c+\coth\chi_p'(b-c)]}\frac{\nu_m\chi_p}{\nu_m'^2+\chi_p^2}.$$

The procedure developed for determining the slab-on-grade solution is also used here. First, the Fourier coefficients f_p and g_p are determined by truncating the sums in equation (20), and in equation (22) to $N = 20$ terms. A system of $2N$ equations with $2N$ unknowns ($f_1, f_2, \ldots, f_N$ and $g_1, g_2, \ldots, g_N$) is obtained. After solving this system using the Gauss–Jordan elimination method, the temperatures inside zones (I), (II), and (III) are determined by substitution of the values of the coefficients f_p and g_p into equations (16)–(18), respectively.

4.1. *Soil temperature variation*

Figure 6(a) shows the wintertime temperature profile around a basement of width $2a = 6$ m and of depth $c = 2$ m. The interior basement temperature is $T_i = 18°C$, and the mean and the amplitude of the annual soil surface temperature variation are $T_m = 8°C$ and $T_v = 7°C$, respectively. A water table at $T_w = 10°C$ is $b = 5$ m below grade. The insulation at the walls and the floor are such that $h_{wl} = 0.2$ W m^{-2} °C^{-1} and $h_f = 1$ W m^{-2} °C^{-1}. The soil thermal diffusivity is $\kappa_s = 6.45 \times 10^{-7}$ m^2 s^{-1}. For this basement configuration, the temperature along the wall increases from 1°C (the wintertime soil surface temperature) to about 11°C; meanwhile, the floor temperature decreases from the central area (16°C) to the edges (11°C). The wall loses heat mostly to the soil surface but the floor heat loss goes entirely to the water table.

Figure 6(b) illustrates the summertime temperature variation for the above basement configuration. Near the wall, the soil temperature decreases from 15°C (the summertime soil surface temperature) to about 13°C. Just beneath the basement floor, the temperature profile is similar to that observed in wintertime (Fig. 6(a)). This is to be expected since there is a strong thermal interaction between the water table and the center of the floor, which is not much affected by the temperature variation with time occurring at the soil surface.

4.2. *Total heat loss calculations*

The complex amplitude of the total heat losses from the floor $\mathscr{Q}_f(\delta)$ and from the wall $\mathscr{Q}_{wl}(\delta)$ are obtained by integrating $\mathscr{I}_f(x) = h_f(\mathscr{T}(x, c) - \mathscr{T}_i)$ and $\mathscr{I}_{wl}(y) = h_{wl}(\mathscr{T}_i - \mathscr{T}(\pm a, y))$ over $[-a, a]$ and $[0, b]$, respectively. It is found that

$$\mathscr{Q}_f(\delta) = -\frac{4}{a} h_f \sum_{n=1}^{\infty} \frac{(-1)^n}{\mu_n} A'_n \tag{23}$$

and

$$\mathscr{Q}_{wl}(\delta) = \frac{2}{c} h_{wl} \sum_{n=1}^{\infty} \frac{[1-(-1)^n]}{\zeta_n} D'_n. \tag{24}$$

with

$$A'_n = \frac{(-1)^n}{[H_f + \mu'_n \coth \mu'_n(b-c)]} \left[\frac{\mu'_n \coth \mu'_n(b-c)}{\mu_n} \mathscr{T}_i - \frac{\mu'_n}{\mu_n \sinh \mu'_n(b-c)} \mathscr{T}_w - \frac{2}{(b-c)} \sum_{m=1}^{\infty} \frac{\mu_n \nu_m}{\mu_n^2 + \nu_m'^2} f_m \right]$$

and

$$D'_n = \frac{1}{[H_{wl} + \zeta'_n \coth \zeta'_n(L-a)]} \times \left\{ \frac{[1-(-1)^n]\zeta'_n \coth \zeta'_n(L-a)}{\zeta_n} \mathscr{T}_i - \frac{C_n \zeta'_n}{\sinh \zeta'_n(L-a)} + \frac{\zeta_n}{\zeta'_n} \mathscr{T}_i \tanh \zeta'_n \frac{(L-a)}{2} + \frac{2}{(L-a)} \sum_{m=1}^{\infty} \frac{(-1)^n \chi_m \zeta_n}{\zeta_n^2 + \chi_m'^2} g_m \right\}.$$

The time-dependent total heat losses from the basement floor $Q_f(t)$ and from the basement wall $Q_{wl}(t)$ are calculated using an equation similar to equation (2)

$$Q_f(t) = \mathscr{Q}_f(0) + \mathrm{Re}[\mathscr{Q}_f(\delta) e^{i\omega t}] \tag{25}$$

and

$$Q_{wl}(t) = \mathscr{Q}_{wl}(0) + \mathrm{Re}[\mathscr{Q}_{wl}(\delta) e^{i\omega t}]. \tag{26}$$

The same basement configuration as in Section 4.1 but with $h_{wl} = 2$ W m^{-2} °C^{-1} is adopted here as the base case to analyze the effect of the water table depth and the insulation level of the walls and floor on the total basement heat losses. The losses from the walls and those from the floor will be analyzed separately.

4.2.1. *Effect of water table depth.* Figures 7(a) and (b) show the annual variation of total heat losses from the basement wall and basement floor, respectively. It is clear that the effect of the water table on floor heat loss is more significant than the effect on wall heat loss. Decreasing the water table level increases the mean annual floor heat loss but decreases the annual fluctuation of total floor heat losses as was observed earlier in the case of a slab-on-grade floor. For the walls, only the amplitude of total heat loss is affected, and only slightly, by water table depth.

4.2.2. *Effect of wall insulation level.* The wall insulation level significantly affects both wall and floor heat losses. For the wall, the mean and the amplitude of total heat losses decrease with h_{wl} as shown in Fig. 8(a). For the floor, only the mean of annual total heat loss is affected significantly by the wall insulation level, as illustrated in Fig. 8(b). The amplitude is essentially unaffected.

4.2.3. *Effect of floor insulation level.* Figure 9(a) shows that the value of h_f affects both the mean and the amplitude of total floor heat losses. Note that the phase lag between soil surface temperature and floor heat loss increases with floor insulation level. Figure 9(b) indicates clearly that the value of h_f has no significant effect on the heat loss from walls.

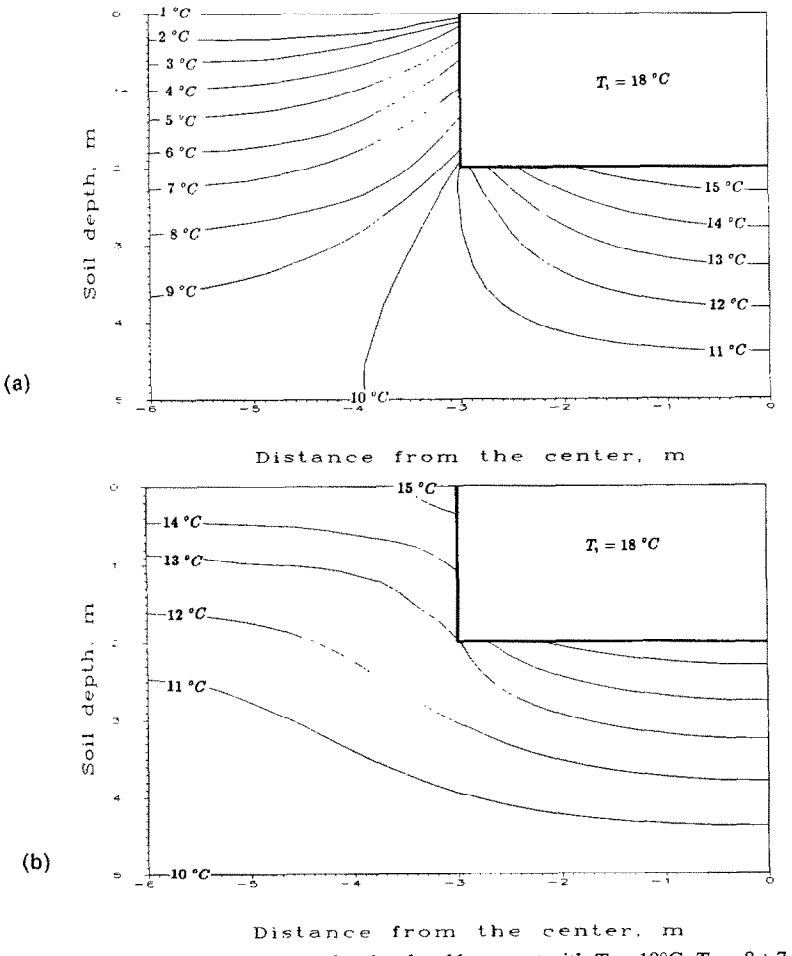

FIG. 6. Earth temperature isotherms around an insulated basement with $T_i = 18°C$, $T_1 = 8+7\cos\omega t$ (°C), $T_w = 10°C$, $H_f = 1\ m^{-1}$, $H_{wl} = 0.2\ m^{-1}$ for: (a) wintertime (15 January); (b) summertime (15 July).

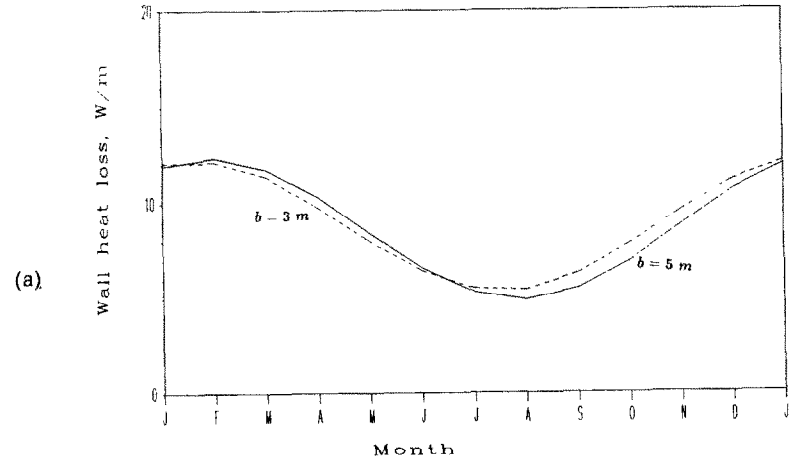

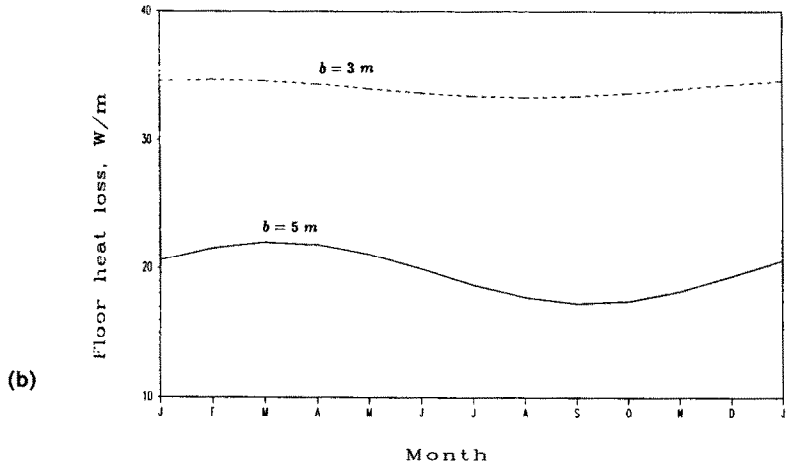

FIG. 7. Effect of water table depth on the annual variation of total heat losses from: (a) basement wall; (b) basement floor.

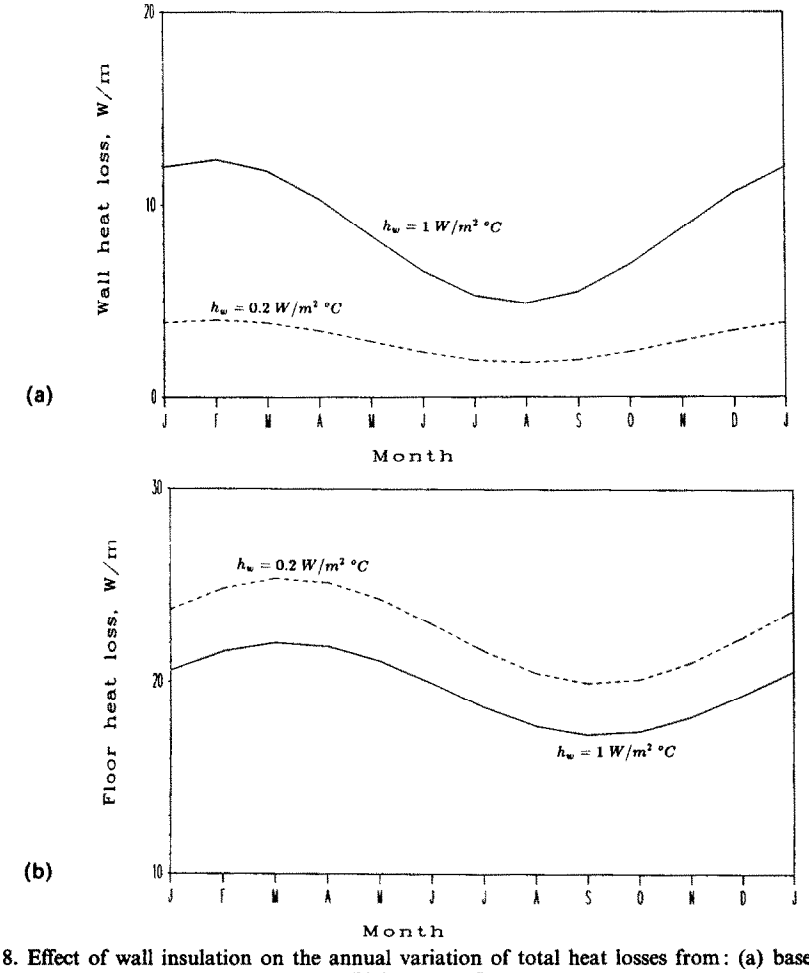

FIG. 8. Effect of wall insulation on the annual variation of total heat losses from: (a) basement wall; (b) basement floor.

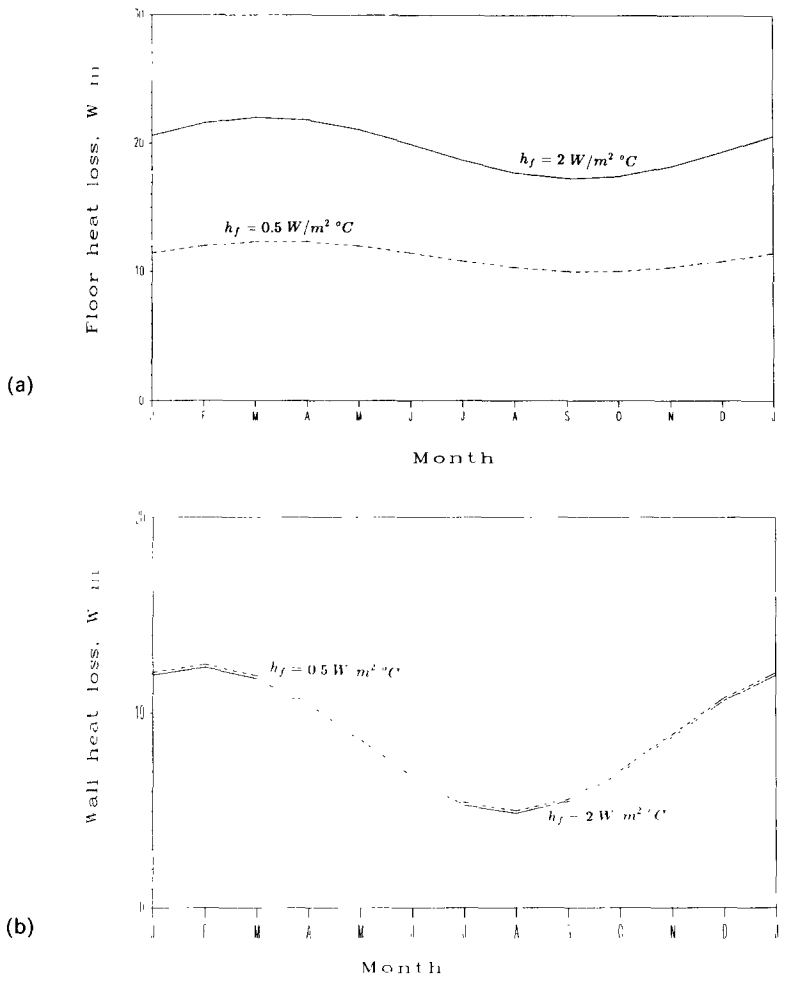

FIG. 9. Effect of floor insulation on the annual variation of total heat losses from: (a) basement floor; (b) basement wall.

5. CONCLUSIONS

A detailed analysis of the heat exchanged between soil and slab-on-grade floors and basements has been carried out using the ITPE technique. The soil temperature variation, the heat flux along each building surface in contact with earth and the total amount of heat flowing into or out of a building envelope is determined in each case. Through parametric analyses, many results are obtained. In particular, we have shown that the isolation effect of the insulation is marked by a time delay to outside fluctuations and that in case of basements the floor has a high thermal sensitivity to the wall insulation. This sensitivity is not mutual since the walls have no significant response to floor insulation.

Throughout this paper, the building envelope is considered as a simple resistance with no capacity. As a consequence, there was no differentiation between inside and outside insulation placement. Further work taking into account heat conduction inside the building envelope material is needed to determine the effect of the insulation placement on heat transfer from buildings to ground. The same work will allow evaluation of the *mass effect* of the envelope material. The ITPE procedure may be utilized to solve the heat conduction equation in both earth and the building envelope.

Acknowledgement—A portion of this work was performed under a Grant-in-Aid awarded to Moncef Krarti by the American Society of Heating Refrigerating and Air Conditioning Engineers. This support is gratefully acknowledged.

REFERENCES

1. M. Krarti, D. E. Claridge and J. F. Kreider, The ITPE technique applied to steady-state ground-coupling problems, *Int. J. Heat Mass Transfer* **31**, 1885–1898 (1988).
2. T. Kusuda and P. R. Achenbach, Earth temperatures and thermal diffusivity at selected stations in the United States, NBS Report 8972, U.S. Government Printing Office, Washington, DC (1965).

3. K. Labs, Underground building climate, *Solar Age* **4:10**, 44–50 (1979).
4. H. S. Carslaw and J. C. Jaeger, *Conduction of Heat in Solids*. Oxford University Press, London (1959).
5. J. H. Chang, *Ground Temperature*, Vols I and II. Bluehill Meteorological Observatory, Havard University (1958).
6. J. M. Akridge and J. F. J. Poulos, The decremented average ground temperature method for predicting the thermal performance of underground walls, *ASHRAE Trans.* **89**(2A), 49 (1983).
7. R. L. Sterling and G. D. Meixel, Review of underground heat transfer research. In *Earth Sheltered Performance and Evaluation Proceedings*, Second National Technical Conference (Edited by L. L. Boyer), pp. 67–74. Oklahoma State University (1981).
8. D. E. Claridge, Design methods for earth-contact heat transfer. In *Advances in Solar Energy* (Edited by K. Boer), pp. 305–344. American Solar Energy Society, Boulder, Colorado (1986).
9. L. S. Shen and J. W. Ramsey, A simplified thermal analysis of earth-sheltered buildings using a Fourier-series boundary method, *ASHARE Trans.* **89**(1B), 438–448 (1983).
10. A. E. Delsante, A. N. Stockes and P. J. Walsh, Application of Fourier transforms to periodic heat flow into the ground under a building, *Int. J. Heat Mass Transfer* **26**, 121–132 (1983).
11. M. Krarti, D. E. Claridge and J. F. Kreider, Interzone temperature profile estimation—slab-on-grade heat transfer results. In *Heat Transfer in Buildings and Structures*, HTD-41, pp. 11–20. ASME, New York (1985).
12. M. Krarti, D. E. Claridge and J. F. Kreider, Interzone temperature profile estimation—below grade basement heat transfer results. In *Heat Transfer in Buildings and Structures*, HTD-41, pp. 11–20. ASME, New York (1985).
13. D. A. DeVries, Thermal properties of soils. In *Physics of Plant Environment* (Edited by R. R. Van Wijk), pp. 210–231. North-Holland, Amsterdam (1963).

APPLICATION DE LA TECHNIQUE ITPE A DES PROBLEMES BIDIMENSIONNELS VARIABLES DE COUPLAGE AU SOL

Résumé—La procédure d'Estimation du Profil de Température Interzone (ITPE) est utilisée pour trouver les solutions en séries analytiques bidimensionnelles des transferts thermiques variables entre le sol et les semelles ou les fondations. La température non perturbée du sol est approchée par une fonction sinusoïdale du temps et la procédure ITPE est couplée avec la technique de la température complexe pour obtenir les solutions périodiques établies dans les deux configurations. On traite analytiquement pour la première fois l'influence de l'isolation et de la nappe d'eau à température fixée sur le comportement temporel des semelles et des fondations.

ANWENDUNGEN DER ITPE-TECHNIK BEI INSTATIONÄREN ZWEIDIMENSIONALEN ERDBODEN-MODELLEN

Zusammenfassung—Die ITPE-Methode (Interzone Temperature Profile Estimation) wird angewandt, um zwei-dimensionale analytische Reihen-Lösungen für die zeitlich veränderliche Wärmeübertragung zwischen Erdboden und oberflächengleichen Böden oder Kellern zu ermitteln. Die ungestörte Bodentemperatur wird als sinusförmige Zeitfunktion angenähert und die ITPE-Prozedur wird mit der komplexen Temperatur-Technik verbunden, um die stetig-periodischen Lösungen für beide Konfigurationen zu ermitteln. Der Einfluß einer Wärmedämmung und einer wasserführenden Schicht konstanter Temperatur auf das zeitliche Verhalten von oberflächengleichen Böden und von Kellern wird erstmalig analytisch behandelt.

ИСПОЛЬЗОВАНИЕ МЕТОДА ОМПТ ДЛЯ РЕШЕНИЯ НЕСТАЦИОНАРНЫХ ДВУМЕРНЫХ ЗАДАЧ ТЕПЛООБМЕНА ОБЬЕКТОВ С ЗЕМЛЕЙ

Аннотация—Метод определения межзонального профиля температур (ОМПТ) используется для получения двумерных аналитических решений в виде рядов для задач нестационарного теплообмена между землей и настилами из плит на уровне земли или подвалами. Невозмущенная температура почвы аппроксимируется синусоидальной функцией времени. С использованием метода ОМПТ получены стационарно-периодические решения для обоих случаев. Впервые аналитически рассмотрено влияние изоляции и грунтовых вод с фиксированной температурой на нестационарные характеристики указанных объектов.